

New observations concerning magnetism and superconductivity in heavy-fermion metals

F. Steglich*, P. Gegenwart, C. Geibel, R. Helfrich, P. Hellmann, M. Lang, A. Link, R. Modler, G. Sparn, N. Büttgen, A. Loidl

Institut für Festkörperphysik, TH Darmstadt, Hochschulstr. 8, D-64289 Darmstadt, Germany

Abstract

Ce-based heavy-fermion superconductors (HFSC) exhibit magnetic phase diagrams differing from those of both the ideal Kondo lattice and substitutional alloys with intact Ce sublattice. While for the Ce-based HFSC (with well localized 4f shell) superconductivity and antiferromagnetic order seem to compete with each other, both phenomena typically coexist for U-based HFSC (with less localized 5f shell).

1. Introduction

Lanthanide- and actinide-based heavy-fermion (HF) compounds behave similarly with respect to their specific-heat (C), susceptibility (χ) and resistivity (ρ), measured well below a characteristic temperature T^* (≈ 10 K). All these quantities reflect the properties of an extremely “heavy” Fermi liquid (FL), i.e. $C = \gamma T$, $\chi \cong \text{const}$ and $\Delta\rho = aT^2$, with coefficients $\gamma \sim \chi \sim \sqrt{a}$ being up to several hundred times larger than in simple metals. Correspondingly large effective quasi-particle masses (m^*) are estimated from the experimental results. A few HF compounds are low- T superconductors (SC). Superconducting (sc) properties like the specific-heat jump at T_c , ΔC , being as gigantic as the normal (n)-state specific heat γT_c , suggest that Cooper pairs are formed by those massive quasi-particles [1].

For most of the HFSC (UBe₁₃ being a seeming exception), cooperative magnetism, usually some kind of antiferromagnetic (afm) ordering, was observed in the

“vicinity” of superconductivity: In the case of U-based compounds the two phenomena antiferromagnetism and superconductivity coexist on a microscopic scale, while they seem to compete with each other in the Ce counterparts. This difference adds to a number of well-known phenomenological differences between U- and Ce-based HF compounds, e.g. in photoelectron spectroscopy, inelastic neutron-scattering and Fermi-surface investigations [2]. There is a long-lasting debate on how to relate these observations to differences in the electronic 5f and 4f structures of the respective U and Ce ions. For lanthanide compounds, the hybridization of their well localized 4f electrons with valence electrons from ligand atoms should, in general, be much weaker than for compounds of the light actinides, having less localized 5f electrons. Consequently, the former are often described within the framework of the “Kondo-lattice” (KL) model, in which charge fluctuations between the 4f shell and the conduction band are ignored [3], while more general schemes, invoking intermediate 5f valence or even itinerant 5f states, are required to understand the physics of actinide-based HF compounds. Before addressing this issue in Section 4, we will investigate in the two subsequent

* Corresponding author.

sections to which extent Ce-based HF compounds meet the expectations for the KL model. Concluding remarks are given in Section 5.

2. Magnetic–nonmagnetic transition and pressure-induced superconductivity in a Kondo lattice: $\text{Ce}(\text{Cu}_{1-x}\text{Ni}_x)_2\text{Ge}_2$ versus CeCu_2Ge_2

For a KL system, the formation of a Néel state via the RKKY intersite interaction (binding energy $k_B T_{\text{RKKY}}$) competes with the formation of a local Kondo singlet (binding energy $k_B T^*$) [3]. These energies depend differently on the same scaling parameter $g = N_{\text{F}}|J|$: $T_{\text{RKKY}} \sim g^2$ and $T^* \sim \exp(-g^{-1})$. Here N_{F} is the conduction-band density of states at the Fermi level and $J < 0$ the local 4f-conduction electron exchange integral. The size of $|J|$ is determined by the corresponding wavefunction overlap. At large cell volume (weak hybridization), the energy gain on forming the Néel state exceeds the one associated with the formation of the Kondo singlet. In this case the Néel state is built by local (somewhat reduced) 4f moments, whereas for $T_{\text{RKKY}} \lesssim T^*$ itinerant models may be more appropriate (“heavy-fermion band magnetism”). In this regime, the magnetic ordering temperature T_{N} is steadily depressed on increasing the parameter g and eventually vanishes at a critical value, g_c .

At sufficiently strong coupling ($g > g_c$, $T^* \gg T_{\text{RKKY}}$), the properties of a coherent FL are expected below some crossover temperature T_{coh} above which paramagnetic 4f moments should be recovered [4, 5]. The existence of a “quantum critical point” for $g = g_c$ ($T_{\text{N}} \rightarrow 0$ K), where the electronic quasi-particles interact with long-range, long-lived magnetic fluctuations [4, 5], manifests itself by non-Fermi-liquid (NFL) effects in the thermodynamic and transport properties. Though other reasons, e.g. a multichannel Kondo-impurity effect [6], could also lead to NFL behavior in these materials, the existence at the quantum critical point in the magnetic phase diagram of the KL could be demonstrated with several concentrated Ce-systems, notably $\text{CeCu}_{6-x}\text{Au}_x$ [7].

Fig. 1 shows (a simplified version of) the magnetic phase diagram of $\text{Ce}(\text{Cu}_{1-x}\text{Ni}_x)_2\text{Ge}_2$ [8], compared to that of undoped CeCu_2Ge_2 under hydrostatic pressure p [9]. We can translate the critical pressure, $p_c = 71$ kbar, at which $T_{\text{N}} \rightarrow 0$ K [9] into a critical cell volume $V_c \cong 167 \text{ \AA}^3$ (upper scale), i.e. by employing the bulk modulus $B \cong 1.2$ Mbar determined at ambient pressure for the homologue CeCu_2Si_2 [10]. This agrees surprisingly well with the cell volume of CeCu_2Si_2 at ambient pressure. On the other hand, the nonmagnetic HF compound CeNi_2Ge_2 exhibits $V \cong 170 \text{ \AA}^3$. Antiferromagnetic order seems to disappear in $\text{Ce}(\text{Cu}_{1-x}\text{Ni}_x)_2\text{Ge}_2$ at

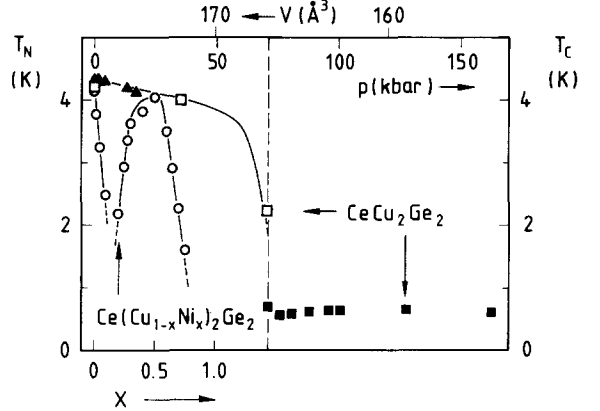


Fig. 1. Magnetic order temperature T_{N} of $\text{Ce}(\text{Cu}_{1-x}\text{Ni}_x)_2\text{Ge}_2$ (○) as a function of Ni-concentration x (bottom scale) [8] and of CeCu_2Ge_2 (▲: $\chi(T)$, □: $\rho(T)$ [9]) as a function of pressure (top inner scale). Superconducting transition temperature T_{c} of CeCu_2Ge_2 (■) as a function of pressure (top inner scale). Bottom scale x is changed into (top outer) volume scale via X-ray diffraction analysis of the lattice parameters, while the (top inner) pressure scale is changed into the (top outer) volume scale by employing the bulk modulus of CeCu_2Si_2 [10].

a critical Ni concentration, $x_c \cong 0.8$. Obviously, along with the steric effect, Ni substitution causes chemical effects, i.e. a locally different electronic structure and hybridization, giving rise to a magnetic phase diagram which is much more complex than that of CeCu_2Ge_2 under pressure.

Let us address the $\text{Ce}(\text{Cu}_{1-x}\text{Ni}_x)_2\text{Ge}_2$ system first. In a previous study [8], an alloying-induced crossover from Ce-derived local-moment ($x < 0.2$) to itinerant HF magnetism ($x \geq 0.5$) was postulated. The latter state was characterized by a rather short incommensurate modulation wave vector and a staggered moment μ_s , which decreases gradually upon increasing Ni concentration. At $x = 0.65$, μ_s was estimated to be smaller than $0.2\mu_{\text{B}}$. No phase-transition anomalies were resolved for alloys with $0.75 < x < 0.8$, indicating further moment reduction when approaching the critical Ni concentration $x_c \cong 0.8$. All available evidence suggests that the quantum phase transition as a function of x is of second order. In the main part of Fig. 2, new results are presented for the temperature dependence of the spin-lattice relaxation rate, T_1^{-1} , determined through ^{63}Cu -NMR experiments on $\text{Ce}(\text{Cu}_{1-x}\text{Ni}_x)_2\text{Ge}_2$ with nearly critical Ni concentration $x = 0.8$ [11]. T_1^{-1} shows a logarithmic increase over one decade in temperature, in agreement [12] with a recent scaling approach in the vicinity of the quantum critical point for the KL. Preliminary specific-heat results on another sample with the same

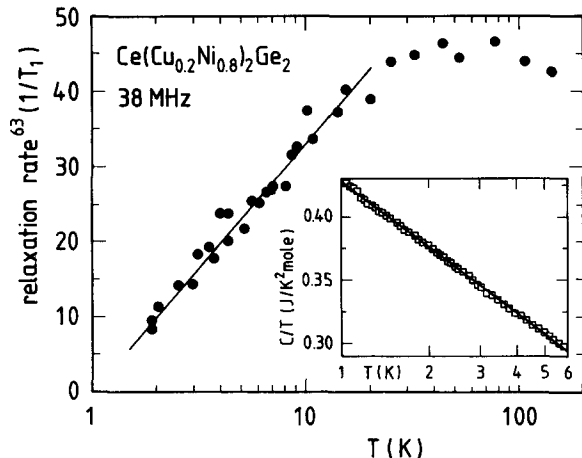


Fig. 2. ^{63}Cu spin-lattice relaxation rate as a function of T (on a logarithmic scale) for $\text{Ce}(\text{Cu}_{0.2}\text{Ni}_{0.8})_2\text{Ge}_2$ [11]. According to Ref. [12], $T_1^{-1} \sim T^{0.3} \ln(T/T_0)$ in the vicinity of the magnetic-nonmagnetic transition. The straight line is a guide to the eye. The inset shows the specific-heat coefficient C/T versus T (on a logarithmic scale) for $\text{Ce}(\text{Cu}_{0.2}\text{Ni}_{0.8})_2\text{Ge}_2$.

composition, shown in the inset of Fig. 2, are consistent with $C/T \sim \ln(T_0/T)$ and thus confirm the NFL effects in T_1^{-1} versus T .

So far, the existence of NFL phenomena on the brink of afm order could qualitatively be verified only with systems exhibiting an intact Ce-sublattice and substitutional disorder on non-f lattice sites. However, disorder may severely change the properties at the quantum critical point [13]. Therefore, hydrostatic-pressure studies on undoped compounds like CeCu_2Ge_2 are of great relevance. In particular, it was of interest to check whether the breakdown of antiferromagnetism in this Ge homologue to CeCu_2Si_2 gave birth to HF superconductivity which does occur neither in CeNi_2Ge_2 nor in the Ni-rich $\text{Ce}(\text{Cu}_{1-x}\text{Ni}_x)_2\text{Ge}_2$ alloys. This expectation was, in fact, met by the discovery of Jaccard et al. [9], who observed for $p \geq p_c = 71$ kbar a sc transition in the resistivity curves taken in a tungsten-carbide Bridgman cell, see Fig. 1. Recent work by Kitaoka et al. [14] demonstrates the existence of this pressure-induced sc state up to $p = 170$ kbar (Fig. 1).

Compared to $T_N(x)$ in the alloy system, the Néel temperature of CeCu_2Ge_2 drops abruptly in the vicinity of the critical pressure, strongly suggesting that the quantum phase transition as a function of pressure is of first order. This resembles the case of CeRh_2Si_2 where $T_N(p)$ disappears suddenly at $p_c \cong 9$ kbar, and a sc transition was recently discovered below 0.4 K at $p > p_c$ [15]. Like in CeRh_2Si_2 [16], no NFL effects are resolved for CeCu_2Ge_2 at the breakdown of antiferromagnetism [9].

In addition, no increase in $T_{\text{coh}}(p)$ as expected in the one-parameter-scaling model [4, 5] can be observed for CeCu_2Ge_2 . Rather T_{coh} , the temperature which limits the validity range of the FL-type T^2 law in the resistivity was found to decrease by more than a factor of two upon increasing the pressure from $p_c = 71$ kbar to $p = 101$ kbar [9]. Here $T_{\text{coh}} \cong 0.7$ K almost coincides with T_c , which may indicate an interesting competition between coherent FL and HF superconductivity; the latter being favored at low magnetic field, while FL effects become visible above the upper critical field, $B_{c2}(T)$ [9].

Another homologue to CeCu_2Si_2 , CePd_2Si_2 , was recently discovered by the Cambridge group [17] to show p -induced HF superconductivity below $T_c \cong 0.4$ K. Above $T = 1.5$ K, the temperature limit accessible in their cryostat, T_N varies linearly with $(p_c - p)$. A critical pressure $p_c \cong 27$ kbar is extrapolated from these data. Unlike CeCu_2Ge_2 , the n -state resistivity of CePd_2Si_2 at $p \cong p_c$ shows NFL behavior in that, within a wide T window, it depends linearly on $T^{1.2}$. Most interestingly, a diamagnetic signal in the AC susceptibility is observed already for $p = 22$ kbar, i.e. in the afm regime. A corresponding feature was noticed in the $\rho(T)$ curves for CeCu_2Ge_2 taken at $p = 62$ kbar, i.e. below the critical value $p_c = 71$ kbar [9]. Future work will have to clarify whether these findings are related to pressure gradients which might cause a heterogeneous mixture of sc and afm regions in the samples. We anticipate that superconductivity does not coexist with antiferromagnetism but rather expels it at these low temperatures, cf. the discussion of CeCu_2Si_2 in the subsequent section.

3. The effect of composition on the ground state of CeCu_2Si_2

We begin this paragraph by recalling that the critical cell volume, $V_c \cong 167 \text{ \AA}^3$, at which in CeCu_2Ge_2 antiferromagnetism becomes suppressed, is nearly identical with the cell volume of CeCu_2Si_2 at ambient pressure. This suggests that in CeCu_2Si_2 (i) some magnetically ordered state may form and (ii) HF superconductivity may occur on the brink of magnetism. Both issues will be briefly addressed below.

Some as-grown single crystals of CeCu_2Si_2 , which forms peritectically, were found to be lacking bulk superconductivity. Instead, a broadened mean-field type of phase transition at $T_A = 0.6\text{--}0.8$ K was observed in their thermodynamic properties [18]. This phase transition is related to distinct anomalies in magnetic properties, i.e. magnetoresistance [19], NMR [20] and μSR [21]. Thus, it is associated by most researchers with some magnetically ordered state, frequently called “phase A”. Up to

now its structure could, however, not be established. Following a special heat treatment in Cu vapor [22], CeCu_2Si_2 single crystals typically are bulk SC below $T_c \cong 0.65$ K. Neither specific-heat nor thermal-expansion results on such “S-type” crystals show any indication of the A-phase transition at $B < 5$ T [18, 2]. Recently, Bruls et al. [23] found that, while annealing is apt to “switch” the ground state of CeCu_2Si_2 single crystals from “A-type” to “S-type”, yet another kind of behavior can occur in high-quality annealed crystals (“AS type”): Upon cooling such a crystal in zero magnetic field, the broadened transition into phase A starts at $T \cong 1.5$ K; before being completed, however, it is replaced at $T_c = T_A$ by a bulk sc transition. For $B > B_{c2}$, phase A is recovered [24], whereas at fields above $\cong 6$ T a new high-field phase (“B”) forms [23].

As the ground state of CeCu_2Si_2 single crystals depends so critically on preparation and annealing conditions, it is likely to be dictated by chemical effects. Unfortunately, standard EMPA and XRD analyses are unsuccessful in resolving significant differences in either the lattice parameters or the compositions of A-, S- and AS-type single crystals, respectively. This was the motivation for Geibel et al. [25] to explore the physical properties of polycrystalline samples with slightly off-stoichiometric compositions. By performing calorimetric and dilatometric experiments they could reproduce all the three kinds of low- T behavior established for CeCu_2Si_2 single crystals [26]. Compared to the unannealed single crystals, “A-type” polycrystalline samples exhibit a further broadening of their A-phase transition. The latter develops gradually below $T \cong 1.5$ K, at which

temperature μSR measurements revealed the formation of magnetic correlations [27]. Fig. 3 displays a small section of the ternary Ce–Cu–Si phase diagram near the stoichiometric 1:2:2 composition. The coexistence regimes between CeCu_2Si_2 and various foreign phases are indicated. Since none of them exhibits significant features below $T \cong 2$ K, the observations made on the various polycrystalline samples reflect the properties of the primary CeCu_2Si_2 phase at the edge of its extremely narrow homogeneity range [28]. As is indicated by different hatchings, the different ground-state properties “A”, “AS”, “S” and the so far unexplored “phase X” [2] can be related to separate sectors of the homogeneity range [25]. Current investigations of the resistivity indicate that the highest crystalline perfection is realized in the “AS” sector where the competing magnetic and sc ground states are almost degenerate. As “driving forces” for these dramatic changes in physical behavior, the occupation of the Cu sublattice [29] and the size of the inplane $4f$ – $5d$ hybridization indicated by the lattice parameter a [18, 30], have been considered.

After having commented on why sc properties of CeCu_2Si_2 are extremely “sample dependent” (a fact that has puzzled researchers since the discovery of HF superconductivity in 1979), we wish to report below some very recent results concerning the “magnetic phase diagram” of this compound:

1. Measurements of both the AC susceptibility and specific heat on an “A-type” polycrystalline sample (Fig. 4) demonstrate that application of a hydrostatic pressure as low as 5 kbar is sufficient to replace its bulk A-phase transition by a bulk sc transition (at $T_c \cong 0.6$ K)

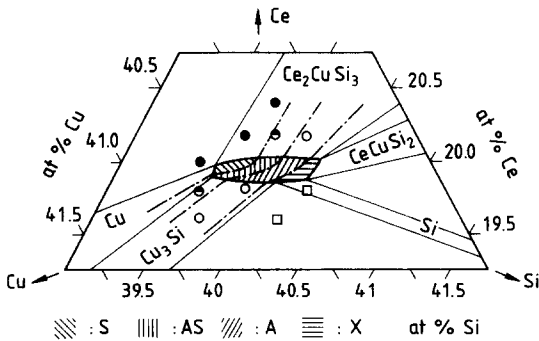


Fig. 3. Proposed qualitative Ce–Cu–Si phase diagram in the vicinity of the stoichiometric “122” composition (dashed: CeCu_2Si_2 homogeneity range). Solid lines indicate mixtures of CeCu_2Si_2 and various foreign phases. Dash-dotted lines separate different physical ground-state properties as determined with polycrystalline samples of different composition: superconductivity “S” (●), phase “A” (○), competition between them “AS” (◐), and phase “X” (□).

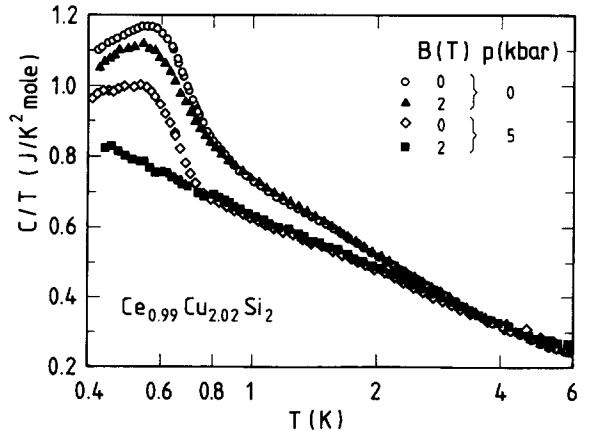


Fig. 4. Specific heat of “A-phase” polycrystalline $\text{Ce}_{0.99}\text{Cu}_{2.02}\text{Si}_2$ sample as C/T versus T (on a logarithmic scale) for $B = 0$ (○) and 2 T (△) at ambient pressure and for $B = 0$ (◇) and 2 T (■) at $p = 5$ kbar, respectively. For $p = 5$ kbar and $B = 0$, the sample is a bulk SC at $T \lesssim 0.6$ k.

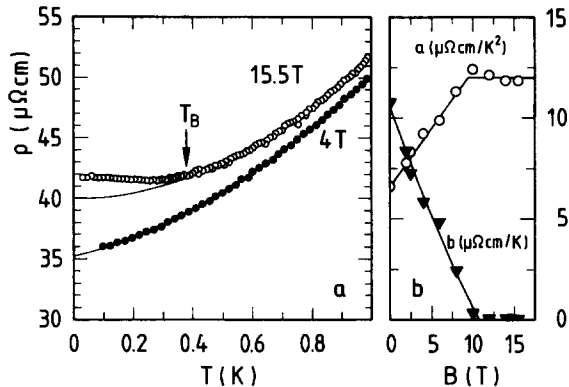


Fig. 5. (a) Temperature dependence of the resistivity of an “S-type” CeCu_2Si_2 single crystal at $B = 4\text{ T}$ and $B = 15.5\text{ T}$. (b) Field dependences of the coefficients in $\rho - \rho_0 = b(B) \cdot T + a(B) \cdot T^2$, see text.

[31]. Furthermore, if pressure-induced superconductivity is suppressed by a B-field of $2T$, C/T is found to vary logarithmically on temperature over more than one decade.

2. The n-state resistivity of an “S-type” single crystal ($T_c = 0.63\text{ K}$) can be well described by $\rho - \rho_0 = bT + aT^2$ (Fig. 5(a)). At zero magnetic field, the “NFL term”, $b(B)T$, dominates over the “FL term”, $a(B)T^2$, whereas the latter takes over upon increasing the field. No contribution linear in T but a huge, field-independent, quadratic contribution is found for $B > 10\text{ T}$ (Fig. 5(b)).

3. For a polycrystalline sample of “A-type” (lacking bulk superconductivity), $\rho - \rho_0 = aT^2$ was observed [2] already at $B = 0\text{ T}$, i.e. below $T = 1.5\text{ K}$, the temperature at which short-range antiferromagnetic Ce–Ce correlations become visible in the μSR experiment [27]. Again the coefficient $a (\cong 10\ \mu\Omega\ \text{cm}\ \text{K}^{-2})$ is gigantic and independent of the B field.

We summarize our present knowledge concerning the magnetic phase diagram of CeCu_2Si_2 as follows: (i) As expected from the pressure studies on CeCu_2Ge_2 [9], HF superconductivity develops on the brink of magnetism (phase A). (ii) Like in the case of CePd_2Si_2 , when exerted to a critical pressure $p_c \cong 27\text{ kbar}$ [17], NFL phenomena show up in the n-state properties of nonmagnetic (“S-type”) CeCu_2Si_2 samples. (iii) While coherent FL phenomena dominate the n-state, low- T resistivity of CeCu_2Ge_2 in the whole nonmagnetic regime ($p \geq p_c$), a huge, field-independent T^2 contribution dominates the resistivity, precursive to the magnetic phase transition in CeCu_2Si_2 .

4. Coexistence of antiferromagnetism and heavy-fermion superconductivity: UNi_2Al_3 versus UPd_2Al_3

In contrast to CeCu_2Si_2 where cooperative magnetism is replaced by HF superconductivity via changes of suitable control parameters (external pressure, composition), U-based HFSC typically show microscopic coexistence of antiferromagnetism and superconductivity at $T \leq T_c < T_N$. Both their sc and afm states exhibit exotic properties. Here, we wish to mention only the discoveries of extremely small staggered moments, $\mu_s = 0.02\ \mu_B$ and $\mu_s = 0.04\ \mu_B$, along with large commensurate ordering wave vectors, for UPt_3 [32] and URu_2Si_2 [33], respectively. The hexagonal HFSC UNi_2Al_3 ($\gamma \cong 120\text{ mJ/K}^2\text{ mol}$, $T_c \cong 1\text{ K}$) orders afm below $T_N = 4.5\text{ K}$ [34]. Its magnetic structure was identified as a longitudinal spin-density wave in which the magnetic moments are polarized within the basal plane [35]. The staggered moment $\mu_s = 0.24\ \mu_B$ [35] coexists with HFSC. Not only the size of μ_s , but also the negative pressure derivative of T_N [36] (Fig. 6) differs greatly from both UPt_3 ($dT_N/dp \cong 0$) and URu_2Si_2 ($dT_N/dp > 0$). A negative pressure derivative of the sc transition temperature as displayed by the specific-heat results of UNi_2Al_3 (Fig. 6) has also been observed for all previously known U-based HFSC [37]. The similar responses of T_c and T_N to external pressure suggest a substantial interaction between HF superconductivity and antiferromagnetism in UNi_2Al_3 .

On turning now to the HF compound UPd_2Al_3 ($\gamma \cong 140\text{ mJ/K}^2\text{ mol}$), the Pd homologue of UNi_2Al_3 , we first note a reinforcement of magnetic properties (presumably associated with a 4.5% increase in cell volume [38]); the Néel temperature being 14.5 K [38] and the staggered moment $0.85\ \mu_B$ [39]. Most interestingly, not only antiferromagnetism but also superconductivity sets in at a much higher temperature than in UNi_2Al_3 . Below

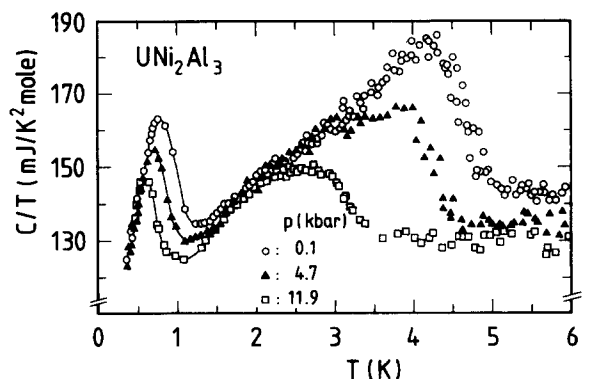


Fig. 6. Specific heat of UNi_2Al_3 at $p = 0.1, 4.7,$ and 11.9 kbar as C/T versus T for $0.4\text{ k} \leq T \leq 6\text{ K}$ [36].

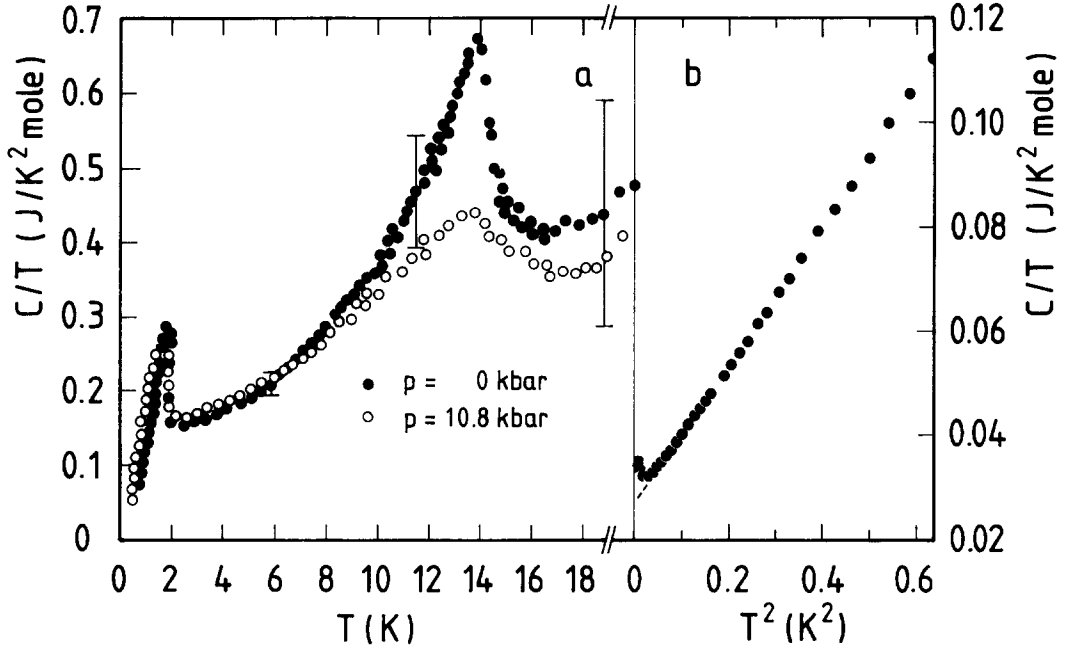


Fig. 7. Specific heat of UPd_2Al_3 as C/T versus T at $p = 0$ and 10.8 kbar for $T \leq 20$ K (a) and at $p = 0$ kbar, well below $T_c = 2$ K, as C/T versus T^2 (b). Vertical error bars in (a) indicate uncertainty in accuracy, associated with the heat capacity of the pressure cell, the error bars in (b) are given by the symbol size. The dashed line in (b) marks C/T after subtraction of the low-temperature upturn which is presumably related to a quadrupolar splitting of ^{27}Al nuclear states.

$T_c = 2$ K [38], microscopic coexistence between these two ordered states was confirmed by neutron-diffraction [39] and μSR [40] experiments. Polarized-neutron studies provided convincing evidence that the magnetic moments are 5f derived [41], i.e. appear as seemingly “local 5f moments”. Furthermore, the sc state is carried by heavy fermions, i.e. “itinerant 5f electrons”. The specific-heat results in Fig. 7 display two hallmarks of HF superconductivity, a huge jump ΔC at T_c , scaling with the large γT_c (Fig. 7(a)) and a nonexponential T -dependence at $T \lesssim 0.5 T_c$ (Fig. 7(b)) [42]. The low-temperature upturn in $C(T)/T$ presumably reflects quadrupolar splitting of nuclear ^{27}Al states. If this is subtracted from the data of Fig. 7(b), one arrives at a residual (as $T \rightarrow 0$) value γ_r . About half of γ_r seems to be an intrinsic property of UPd_2Al_3 [2]. This intrinsic value, $\gamma_m \approx 15$ $\text{mJ}/\text{K}^2 \text{mole}$, was tentatively ascribed to a subsystem of unpaired 5f states associated with afm order, while $\gamma_s = (\gamma_n - \gamma_m) \approx 125$ $\text{mJ}/\text{K}^2 \text{mole}$ was ascribed to those 5f states forming Cooper pairs [43,44]. Knight-shift results obtained through μSR experiments support this coexistence of seemingly “localized” and “itinerant 5f states” [45]. The two 5f subsystems in UPd_2Al_3 appear to be only weakly coupled to each other:

1. Pressure up to ≈ 11 kbar, while having a strong effect on the afm transition, leaves the sc transition nearly unaffected (Fig. 7(a)). Furthermore, resistivity experiments reveal a linear T_N -depression up to $p \approx 70$ kbar, whereas T_c remains unchanged in this pressure range [46].

2. Alloying with nonisoelectronic dopands (no matter, on which of the three different lattice sites they are substituted, and whether or not they carry a magnetic moment) has the opposite effect. It destroys superconductivity very efficiently, but is harmless to AFM [47].

In summary, we have discussed experimental results on UPd_2Al_3 which hint at two microscopically coexisting 5f subsystems of very different kind: The more localized 5f states appear to cause seemingly “local-moment magnetism”, whereas the less localized ones appear to carry HF superconductivity.

5. Conclusions

Within the last few years, the magnetic phase diagram of the idealized Kondo lattice [3–5] has been qualitatively verified for a couple of *disordered Ce alloys* with undisturbed Ce sublattices. Concerning the non-Fermi-liquid

effects, which are observed near the *antiferromagnetic* quantum phase transition in systems like $\text{CeCu}_{6-x}\text{Au}_x$ [7], it has to be explored by future theoretical work, why the specific heat follows $T \ln(T_0/T)$, while the susceptibility follows a power-law T -dependence [13].

For a few (isostructurally) *ordered Ce compounds*. HF superconductivity shows up on the brink of magnetism. For CeCu_2Ge_2 [9], CeRh_2Si_2 [15,16] and CeCu_2Si_2 magnetic order disappears in an abrupt fashion at a critical value of hydrostatic pressure. Striking discrepancies from the idealized KL phase diagram have been recognized: (1) The normal state of sc CeCu_2Ge_2 , as obtained by applying an overcritical magnetic field, behaves as a coherent FL in the whole pressure regime, including even $p \cong p_c$ [9]. Similar behavior of CeRh_2Si_2 is subject of current investigations [15,16]. (2) For CeCu_2Si_2 , NFL effects are observed to be associated with the suppression of the magnetic phase A. Upon cooling, the latter seemingly develops out of a coherent FL which for a KL should be separated from antiferromagnetism by a quantum critical point [4,5]. These results, along with those in CePd_2Si_2 , which also does exhibit NFL effects near $p = p_c$ [17], call for future investigations concerning the effect of HF superconductivity on the magnetic-nonmagnetic transition in Ce-based HF compounds.

Compared to homogeneous samples (single crystals) of CeCu_2Si_2 , in which antiferromagnetism (phase A) and HF superconductivity seem to expell each other as a function of temperature, magnetic field and pressure, both phenomena typically coexist on a microscopic scale in U-based HF compounds, again in conflict with KL behavior. This remarkable difference in the low-temperature properties of Ce- and U-based HF metals is likely to reflect differences in the $4f/5f$ -states [2]. Therefore, we wish to conclude by emphasizing that the origin of heavy fermions in the U compounds remains yet to be explained. As far as Ce compounds like CeCu_2Si_2 are concerned, a Kondo-type effect is usually held responsible for heavy-fermion formation [1,2]. This interpretation has recently been criticized [48]. Our observation that the prototypical Ce-based HF compounds discussed in this paper show magnetic phase diagrams differing from that of the idealized Kondo lattice [4,5] indicates that the physics of these materials, too, is presently far from being understood.

Acknowledgements

We would like to thank P. Coleman, M.A. Continentino, D.L. Cox, L.P. Gor'kov, J. Kübler, G.G. Lonzarich, B. Lüthi and M.R. Norman for stimulating conversa-

tions. This work was performed within the research program of the SFB 252 Darmstadt/Frankfurt/Mainz.

References

- [1] For a review see, e.g.: N. Grewe and F. Steglich, in: Handbook on the Physics and Chemistry of Rare Earths, Vol. 14, eds. K.A. Gschneidner Jr. and L. Eyring (Elsevier, Amsterdam, 1991) p. 343.
- [2] F. Steglich et al., Proc. Int. Conf. on Physical Phenomena at High Magnetic Fields II, Tallahassee, Florida (1995), in press.
- [3] S. Doniach, Physica B 91 (1977) 231.
- [4] M.A. Continentino et al., Phys. Rev. B 39 (1989) 9734; M.A. Continentino, Solid State Commun. 75 (1990) 89.
- [5] A.J. Millis, Phys. Rev. B 48 (1993-II) 7183.
- [6] D.L. Cox, Phys. Rev. Lett. 59 (1987) 1240; T.-S. Kim and D.L. Cox, Phys. Rev. Lett. 75 (1995) 1622.
- [7] H.v. Löhneysen et al., Phys. Rev. Lett. 72 (1994) 3262; B. Bogenberger and H.v. Löhneysen, Phys. Rev. Lett. 74 (1995) 1016.
- [8] A. Loidl et al., Ann. Physik 1 (1992) 78.
- [9] D. Jaccard et al., Phys. Lett. A 163 (1992) 475; D. Jaccard and J. Sierro, Physica B 206 & 207 (1995) 625.
- [10] I.L. Spain et al., Physica B 139 & 140 (1986) 449.
- [11] N. Büttgen, R. Böhmer and A. Loidl, to be published.
- [12] M.A. Continentino, to be published.
- [13] P. Coleman, Physica B 206 & 207 (1995) 872.
- [14] Y. Kitaoka et al., Physica B 206 & 207 (1995) 55.
- [15] R. Movshovich et al., Physica B 223 & 224 (1996) 126.
- [16] M. Grosche, Dissertation, University of Cambridge (1995), unpublished.
- [17] S.R. Julian et al. to be published; F.M. Grosche et al., Physica B 223 & 224 (1996) 50.
- [18] M. Lang et al., Physica Scripta T 39 (1991) 135.
- [19] U. Rauchschwalbe et al., J. Magn. Magn. Mat. 63 & 64 (1987) 447.
- [20] H. Nakamura et al., J. Magn. Magn. Mat. 76 & 77 (1988) 517.
- [21] Y.J. Uemura et al., Phys. Rev. B 39 (1989) 4726.
- [22] W. Sun et al., Z. Phys. B 80 (1990) 249.
- [23] G. Bruls et al., Phys. Rev. Lett. 72 (1994) 1754.
- [24] The A-S transition is of first order at $B > 0$ T whereas at $B = 0$ T, $T_A = T_c$ marks a tricritical point [R. Modler, Dissertation, TH Darmstadt (1995), unpublished].
- [25] C. Geibel et al., to be published.
- [26] R. Modler et al., Physica B 206 & 207 (1995) 586.
- [27] R. Feyerherm et al., Physica B 206 & 207 (1995) 596.
- [28] The Cu-Si homogeneity range (< 2 at %) was established by EDAX [27], while the perpendicular width (Ce composition) indicated in Fig. 3 is an upper bound dictated by the resolution of XRD [25].
- [29] H. Spille et al., Helv. Phys. Acta 56 (1983) 165.
- [30] D. Finsterbusch et al., Physica B 223 & 224 (1996) 329.
- [31] This agrees with both the estimate of $(\partial T_A / \partial p)_{p=0} \cong -200$ mK/kbar [18] and the observation of p -induced superconductivity in non-sc single crystals at a few kbars [F.G. Aliev et al., Solid State Commun. 47 (1983) 693] and, thus, supports the relevance of the lattice parameter a [18].

- [32] G. Aeppli et al., *Phys. Rev. Lett.* 63 (1989) 676.
- [33] C. Broholm et al., *Phys. Rev. Lett.* 58 (1987) 1467.
- [34] C. Geibel et al., *Z. Phys. B* 83 (1991) 305.
- [35] J.G. Lussier et al., *Physica B* 199 & 200 (1994) 137.
- [36] M. Keller, Diploma Thesis, TH Darmstadt (1994), unpublished.
- [37] J.D. Thompson and J.M. Lawrence, in: *Handbook on the Physics and Chemistry of Rare Earths*, Vol. 19, eds. K.A. Gschneidner et al. (Elsevier, Amsterdam, 1994) p. 383.
- [38] C. Geibel et al., *Z. Phys.* 84 (1991) 1.
- [39] A. Krimmel et al., *Z. Phys. B* 86 (1992) 161; *Solid State Commun.* 87 (1993) 829; H. Kita et al., *J. Phys. Soc. Japan* 63 (1994) 726.
- [40] A. Amato et al., *Europhys. Lett.* 19 (1992) 127.
- [41] L. Paolasini et al., *J. Phys.: Condens. Matter* 5 (1993) 8905.
- [42] The result of Fig. 7(b), $C/T = \gamma_r + \beta T^2$, for $T \leq 0.8$ K, contradicts the NQR result obtained from the same sample, $(T_1 T)^{-1} = DT^2$ [14]; cf. also the paper by P. Coleman et al., *Physica B* 223&224 (1996) 40.
- [43] R. Caspary et al., *Phys. Rev. Lett.* 71 (1993) 2146.
- [44] We again note that no "Korringa term" related to $\gamma_r T$ could, so far, be resolved in the NQR result [14].
- [45] R. Feyerherm et al., *Phys. Rev. Lett.* 73 (1994) 1849.
- [46] P. Link et al., *J. Phys.: Condens. Matter* 7 (1995) 373.
- [47] C. Geibel et al., *Physica B* 199 & 200 (1994) 128.
- [48] L.P. Gor'kov, *Physica B* 223&224 (1996) 241.